REPORT DOCUMENTATION PAGE

Form Approved
OMB No. 0704-0188

PLEASE DO NOT RETURN YOUR FORM TO THE ABOVE ORGANIZATION.

1. REPORT DATE *(DD-MM-YYYY)*	2. REPORT TYPE	3. DATES COVERED *(From - To)*
31-08-2010	Final	01-06-2007 to 31-08-2010

4. TITLE AND SUBTITLE

Self-Configuration and Localization in Ad Hoc Wireless Sensor Networks

5a. CONTRACT NUMBER

FA9550-06-1-0375

5b. GRANT NUMBER

5c. PROGRAM ELEMENT NUMBER

6. AUTHOR(S)

Lance C. Pérez and Stephen Goddard

5d. PROJECT NUMBER

5e. TASK NUMBER

5f. WORK UNIT NUMBER

7. PERFORMING ORGANIZATION NAME(S) AND ADDRESS(ES)

Dept. of Electrical Engineering
University of Nebraska, Lincoln
Lincoln, NE 68588-0511

8. PERFORMING ORGANIZATION REPORT NUMBER

9. SPONSORING/MONITORING AGENCY NAME(S) AND ADDRESS(ES)

Air Force Office of
Scientific Research (AFOSR)

10. SPONSOR/MONITOR'S ACRONYM(S)

AFOSR

11. SPONSOR/MONITOR'S REPORT NUMBER(S)

AFRL-OSR-VA-TR-2012-0159

12. DISTRIBUTION/AVAILABILITY STATEMENT

A

13. SUPPLEMENTARY NOTES

14. ABSTRACT

This project studied the performance of ad hoc wireless sensor networks with respect to communications, event detection and localization. A combination of experiments and simulation were used. The experiments were conducted on a test bed consisting of over 200 sensor nodes. A probabilistic de• nition of connectivity in heterogeneous wireless sensor networks (WSNs) has been developed. Connectivity between two nodes is defined as whether a given packet or a series of packets can be delivered before a speci• c deadline with at least a given probability. Using this de• nition, admission control, routing and other network services considering timing requirements were built. Improvements in embedded system design and low-power wireless communication techniques have enabled the realization of large-scale systems that can directly interact with the environment without any human interaction. These systems are called cyber physical systems. We have developed a cyber-physical system architecture, a novel event-based system design concept, and new theories for reasoning about time and space. Iterative decoding techniques have lead to a class of near-capacity achieving codes called low-density parity check codes. Theoretical constructs were developed to better describe these codes and to enable more accurate prediction of their performance, particularly at the short block lengths used in sensor networks.

15. SUBJECT TERMS

sensor networks, localization, low density parity check codes

16. SECURITY CLASSIFICATION OF:			17. LIMITATION OF ABSTRACT	18. NUMBER OF PAGES	19a. NAME OF RESPONSIBLE PERSON
a. REPORT	b. ABSTRACT	c. THIS PAGE			Lance C. Pérez
none	none	none	none	13	19b. TELEPHONE NUMBER *(Include area code)* 402-472-6258

Reset

Final Report: Self-Configuration and Localization in Ad Hoc Wireless Sensor Networks

Lance C. Pérez and Stephen Goddard

I. Summary of Contributions

We explored the error mechanisms of iterative decoding of low-density parity-check (LDPC) codes. This work has resulted in nine peer-reviewed conference papers [1], [2], [3], [4], [5], [6], [7], [8], [9], three journal papers [10], [11], [12], and two pending journal papers [13], [14] in the fields of channel coding and information theory. The study of iterative decoders and their behavior is one of the most important problems in the area of channel coding, as their unpredictable behavior has impeded the deployment of LDPC codes in many real-world applications. We proposed a theoretical decoder, referred to as a universal cover decoder, that allows connections to be drawn between iterative decoders and other more well-understood decoders like the linear program decoder and graph cover decoder [2], [4]. During our examination of the error-causing mechanisms of iterative decoders, we were able to prove several previously unknown properties related to their behavior [10].

We also developed several finite tree-based decoders of LDPC codes, including the extrinsic tree decoder, and an investigation into their performance and bounding capabilities [5], [6]. This research led to the discovery of a new category of error causing mechanisms, known as deviation-based trapping sets [7], [11]. Preliminary results show that it is possible to use deviation-based trapping sets to conditionally upper bound the probability of error for iterative decoding of LDPC codes [14]. Our work in channel coding and network coding was also applied to wireless sensor networks (WSN). Wireless sensors often require a high level of power-efficiency, and can benefit from network communications strategies that use both channel coding and network coding. We recently created a decoder that integrates non-binary LDPC codes, random linear network coding, and a new correlation decoder that operates on systems where the sensors have correlated data [9]. Preliminary results show that significant improvements can be achieved using this new decoder.

Using these funds a wireless sensor network testbed is developed in the Cyber-Physical Networking Laboratory, Computer Science and Engineering, UNL. The inventory in the lab consists of over 200 sensor nodes including MicaZ, SunSPOT, TMoteSky/TelosB, IRIS, and Imote2 as well as NB100/NSLU2 and HP iPAQ hw6925 gateways; CMUCam3 CMOS cameras and Acroname Garcia Mobile Robots. The CPN Testbed supports remote programming, out-of-band monitoring, power management, and virtual sensing. A management software has been developed using the Linux (XubunTOS) operating system, Bash and PHP scripts, the MySQL database, and the ApacheWeb Server. For the power management support, a hardware/software solution based on the DAQ device NI-6810 (from National Instruments Inc.) and a customized microcontroller control board is being developed so that real-time energy consumption monitoring is supported. Finally, a virtual sensing platform is being designed to emulate sensing readings in a evaluation scenario. The WSN testbed has been intensively used for the purpose of validating the accuracy of various probabilistic QoS analysis models for WSNs. Significant contributions from this work include a new cyber-physical event model [15] and concept lattice-based extensions that facilitate complex event compositions [16].

To provide an analytical tool for the development of real-time WSN solutions, in [17], the distribution of end-to-end delay in multi-hop WSNs is investigated. Accordingly, a comprehensive and accurate crosslayer analysis framework, which employs a stochastic queueing model in realistic channel environments, is developed. This framework captures the heterogeneity in WSNs in terms of channel quality, transmit power, queue length, and communication protocols. To validate the probabilistic analytical framework of the end-to-end delay, realistic experiments with TelosB motes are conducted on the testbed. The experiments are

conducted with varying network parameters and topologies, and the measured delay is used to compare against the model analysis. The cross-layer framework can be used to identify the relationships between network parameters and the distribution of end-to-end delay and accordingly, to design real-time solutions for WSNs. To the best of our knowledge, this is the first work to investigate probabilistic QoS guarantees in WSNs.

In [18], a stochastic analysis of the energy consumption in WSNs is developed for random network deployments. Accordingly, a comprehensive cross-layer analysis framework, which employs a stochastic queueing model, is developed. Using this framework, the distribution of energy consumption for nodes in WSNs during a given time period is found. It is shown that when the time duration is long, the energy consumption asymptotically approaches the Normal distribution. To validate the probabilistic energy consumption analysis for WSNs, data acquisition modules equipped in the testbed are utilized to measure the energy consumption by each node. The battery voltage and the current drawn by the mote are measured over time to obtain the actual power consumption. Since the modules can continuously monitor the voltages at a high frequency of 10kHz, we are able to capture the energy consumption of a packet transmission, which takes less than 2ms. The cross-layer framework is also used to identify relationships between the distribution of energy consumption and network parameters, such as network density, duty cycle, and traffic rate.

Finally, in [19], a spatio-temporal fluid model is developed to capture the delay characteristics of event detection in large-scale WSNs. More specifically, the distribution of delay in event detection from multiple reports is modeled. Accordingly, metrics such as mean delay and soft delay bounds are analyzed for different network parameters. The testbed is used to validate our event detection delay analysis. In the experiment, each node within a certain range simultaneously starts to generate a series of report packets upon receiving a signaling packet. The delay until the first n report packets received by a designated sink is recorded as the event detection delay. This measured delay is used to validate the accuracy of the proposed analytical model. The resulting framework can be utilized to analyze the effects of network and protocol parameters on event detection delay to realize real-time operation in WSNs.

II. Detailed Localization Results

A. Overview of Mobility Models

Movement models can be classified into two broad categories: *entity* models and *group* models. Entity models are used to describe movement of an individual person. This person's movement is independent of outside activities, such as other people's movements. Entity models are widely used in Mobile Ad-hoc NETwork (MANET) simulations. Group models are used to describe the movements of many individuals. Unlike in entity models, an individual's movements are now dependent upon outside activities, such as other individuals' movements. Some scenarios, such as battlefield movement or traffic patterns on a freeway, may be inappropriate for entity modelling. In such cases a group model may be used to more accurately capture movement patterns.

The Random Walk Mobility Model has been a widely used model for individual movements0. Its appeal lies in its simplicity; consider first the simple one-dimensional (1-D) Random Walk model. In this case, the mobile node is able to move forward and backward only, as if he/she were forced to walk along a beam. At equal steps in time, separated by T, the mobile node is allowed to choose a direction and speed randomly from predefined ranges, i.e., [Forward Backward] and [$\mathrm{v}_{\min}$ $\mathrm{v}_{\max}$], respectively. The mobile node then travels in this direction at this speed for time T, at which time it repeats the process of randomly choosing a new direction and speed. In the case of an n-D Random Walk, the only difference is that the node can now move in any direction in the n-D space, rather than simply forward or backward.

Movements in the Random Walk model are independent of each other in time, and are also independent of other mobile nodes' activities. This independence hinders the ability of the model to realistically model a person's movement, since a person's movement at one point in time is typically affected by his/her

previous movement. It would be unrealistic for a person to make completely random movements while trying to get from the living room to the kitchen, for example.

The Random Waypoint model is a slightly modified version of the Random Walk model, and has been used as a 'benchmark' model for the evaluation of MANET routing protocols. In this model, a mobile node still chooses a random speed from a predefined range. However, instead of continuing the selected movement over a period of time T, the node randomly selects a destination within the simulation area, and continues movement until reaching the destination. Once the node has reached the destination, it waits here for a certain period of time (pause time), which can be randomly chosen from a predefined range. After this time expires, the mobile node repeats the process of choosing random movement.

Just as for the Random Walk, this model's movements are independent in time and independent of other nodes' activities. However, this model addresses the unrealistic movement of the Random Walk in moving randomly at equal intervals of time to get from one location to a destination. The Random Waypoint model attempts to model this destination-driven aspect of human movement, which may make it more realistic than the Random Walk model.

An undesired phenomenon appears in the simulation of many nodes making use of the Random Waypoint model, which led to the development of the Random Direction model. The phenomenon is a high probability of nodes traveling to or through the center of the simulation area, which is undesirable when clustering patterns are to be avoided. To alleviate this effect, the Random Direction model requires a node to pick a random direction and speed, and continue traveling in that direction until it reaches a boundary of the simulation area. Once it reaches a boundary, it picks a random pause time, and then repeats the random movement process. A slightly modified version of the Random Direction model allows the node to pick a random destination along its random direction that it has chosen, rather than force it to continue movement to a boundary. It should be noted that this model is equivalent to a Random Walk model with pause times. The Gauss-Markov model attempts to model the fact that human movement is not completely random, but is actually dependent upon previous movements. This model 'tunes' the randomness through one parameter, α.

A node is initially assigned a speed and direction. At fixed intervals in time separated by T, the node calculates its next movement at time nT through

$$S_n = \alpha S_{n-1} + (1-\alpha)\,\mu_S + \sqrt{(1-\alpha^2)}N_S \tag{1}$$

and

$$D_n = \alpha D_{n-1} + (1-\alpha)\,\mu_D + \sqrt{(1-\alpha^2)}N_D, \tag{2}$$

where S_{n-1} and D_{n-1} are the current speed and direction, respectively; $0 \leq \alpha \leq 1$ is the tuning parameter of randomness; μ_S and μ_D are the mean values of speed and direction as $n \to \infty$; N_S and N_D are zero-mean Gaussian random variables with variances σ_S^2 and σ_D^2, and possibly a non-zero covariance, σ_{SD}. Note that when $\alpha = 0$, there is no correlation between the current movement and the next movement, which corresponds to purely random movements which are independent at each point in time. The other extreme is when $\alpha = 1$, where the current movement is identical to the previous movement. This case corresponds to linear movement.

Another model that makes use of non-random movement is the Probabilistic Version of the Random Walk Model (PVRW). By utilizing a transition probability matrix,

$$\mathbf{P} = \begin{bmatrix} \mathrm{P}(0|0) & \mathrm{P}(0|1) & \mathrm{P}(0|2) \\ \mathrm{P}(1|0) & \mathrm{P}(1|1) & \mathrm{P}(1|2) \\ \mathrm{P}(2|0) & \mathrm{P}(2|1) & \mathrm{P}(2|2) \end{bmatrix}, \tag{3}$$

the current movement choice at time nT is affected by past movements. State 0 is the no movement case, state 1 is a movement in the negative direction (x or y axis), and state 2 is a movement in the positive direction (x or y axis). This model produces a movement at time $(n+1)T$ which is dependent

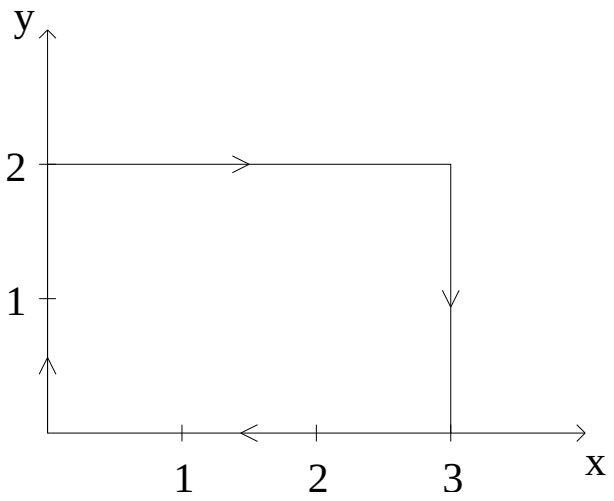

Fig. 1. Rectangular Perimeter.

upon the previous movement at time nT. This may be more realistic than producing a movement that is independent of the previous movement, which results in purely random movements.

People tend to move mostly forward in day-to-day tasks, and it is unusual to have a sudden, backward movement. This model makes use of this pattern of human movement in $\mathbf{P}$, as transition probabilities for movement (given that the node is already moving, e.g., $\mathrm{P}(2|2) = 0.7$) are higher than probabilities of moving directly backward, which in this model, are zero. Although this model may be more realistic, appropriate transition probabilities $\mathrm{P}(i|j)$ are needed. These probabilities must be found from path data of actual human movement. In addition, given that probabilities have been found from actual movement, the values may only be appropriate for the movement scenario from which the data was recorded.

B. A New Mobility Model

The new simulation mobility model proposed here has been named the *Modified Probabilistic Version of the Random Walk* (MPVRW), since it is related to the PVRW model. Recall that the PVRW defined movements using a state transition matrix, $\mathbf{P}$. The transition probabilities defined how the next movement was related to the previous movement, and so the PVRW was a Markov model of the first order. Movements were defined relative to the two axes, x and y, and the PVRW used separate transition matrices for each axis. Consider the x-axis only. The states are forward (2), no movement (0), and backward (1). The transition probabilities say that given state S in the x-axis at time nT:

- the probability of moving in the positive x direction at time $(n+1)T$ is $\mathrm{P}(2|S)$
- the probability of moving in the negative x direction at time $(n+1)T$ is $\mathrm{P}(1|S)$
- the probability of not moving in the x direction at time $(n+1)T$ is $\mathrm{P}(0|S)$

The transition probabilities for the y-axis are defined in the same fashion.

There are some shortcomings of the PVRW model. Realistic transition probabilities are not provided for this model, and only educated guesses have been made. In addition, the sampling interval, T, has not been defined. Lastly, this model assumes that if any movement occurs, it is always the same velocity. In fact, this velocity is simply a preset average velocity in previous work. The MPVRW model is designed to address these shortcomings. The problem of not knowing realistic probabilities is eliminated, as these were derived from movement data of actual human movement. The sampling interval, T, is defined for this model. In order to improve the velocity modelling, the MPVRW model uses probabilities to describe a velocity distribution, rather than assuming constant velocity.

In order to understand the MPVRW, the concept of relative movement must first be introduced. Consider the simple case of a person walking around the perimeter of a rectangle (See Figure 1). The object moves clockwise around the rectangle, beginning and ending at $(0, 0)$, by taking steps of length 1 meter at

each sample time, $nT, n = 0, 1, \ldots, 10$. In terms of absolute movement, this path could be completely described by the positions at each sample time. However, in terms of relative movement, the path would be completely described by the set of relative movements at each sample time, i.e., (forward, forward, right, forward, forward, right, forward, right, forward, forward), where the first movement is assumed to be forward. As seen in this simple example, relative movement defines the current movement *relative* to the previous movement. The movements described by the MPVRW are relative movements, rather than absolute movements, as are used in the PVRW.

The MPVRW has two sets of independent transition probabilities. The first set defines the relative movements, while the second set defines the velocities. Since these are discrete state transitions, the relative movements and velocities must be quantized into discrete values. The number of quantization levels affects the accuracy of the model, but the number of quantization levels is also limited by the finite memory constraints of any computer. For simplicity, only 9 quantization levels will be discussed, but this number has no special importance.

Maintaining consistent notation is important, and so the relative movements are labeled as seen in Figure 2. Forward is always labeled as 1, with the rest of the movements labeled sequentially in a clockwise

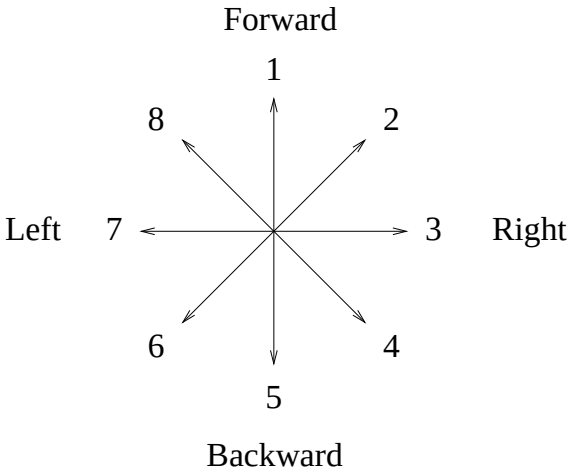

Fig. 2. Quantized Relative Movement Notation.

fashion. In addition, a 'no relative movement' state is included, and is always labeled as the last state (e.g., 9 in this example). For the quantized velocities, 0 m/s is always labeled as 1, and 2 m/s is always labeled as the last state. The remaining quantized velocities are evenly spaced between the two extremes (e.g., $\frac{1}{4}, \frac{1}{2}, \ldots, 1\frac{3}{4}$ m/s), and are labeled $2, 3, \ldots, 8$, respectively.

The first-order transition probabilities for relative movements and velocities are stored in $\mathbf{P}_{M|m_{i-1}}$ and $\mathbf{P}_{V|v_{i-1}}$, respectively. The entries of $\mathbf{P}_{M|m_{i-1}}$ are labeled as

$$\mathbf{P}_{M|m_{i-1}} = \begin{bmatrix} \mathrm{P}_M(1|1) & \cdots & \mathrm{P}_M(1|9) \\ \vdots & \ddots & \vdots \\ \mathrm{P}_M(9|1) & \cdots & \mathrm{P}_M(9|9) \end{bmatrix}, \tag{4}$$

where $\mathrm{P}_M(j|k)$ is the probability of movement j at time iT given movement k at time $(i-1)T$. The entries of $\mathbf{P}_{V|v_{i-1}}$ are labeled as

$$\mathbf{P}_{V|v_{i-1}} = \begin{bmatrix} \mathrm{P}_V(1|1) & \cdots & \mathrm{P}_V(1|9) \\ \vdots & \ddots & \vdots \\ \mathrm{P}_V(9|1) & \cdots & \mathrm{P}_V(9|9) \end{bmatrix}, \tag{5}$$

where $\mathrm{P}_V(j|k)$ is the probability of velocity j at time iT given velocity k at time $(i-1)T$.

In addition to first-order transition probabilities, the MPVRW model can take into account any desired order of probabilities. Of course, if the statistics of realistic movement are not strongly dependent upon higher order probabilities, then they should not be used, as they add complexity to the model. However, if the higher order probabilities are found to be significant, then their use should be considered. This consideration would have to take into account the memory constraints of the system, as the size of the transition matrices grows exponentially with increasing order.

Supposing that b^{th}-order statistics are used, the matrix would have $b+1$ dimensions, and would be denoted by $\mathbf{P}_{M|\mathbf{m}_b}$ and $\mathbf{P}_{V|\mathbf{v}_b}$ for movements and velocities, respectively. Individual entries would have the form $\mathrm{P}_M(m|\mathbf{m}_b)$, which is the probability of movement m at time iT given movements $\mathbf{m}_b = [m_{i-1}, \ldots, m_{i-b}]$ at times $(i-1)T, \ldots, (i-b)T$, respectively. Similar notation is used for velocities.

As mentioned, the MPVRW model assumes that movement and velocity probabilities are independent of each other. However, this assumption may not be true. Therefore a model which makes use of this dependence is proposed, and is called the *Joint* MPVRW (JMPVRW) model. This model is identical to the MPVRW model, with the independent transition probability matrices, $\mathbf{P}_{M|\mathbf{m}_b}$ and $\mathbf{P}_{V|\mathbf{v}_b}$ replaced with a joint transition probability matrix, $\mathbf{P}_{M,V|\mathbf{m}_b,\mathbf{v}_b}$.

Assuming that b^{th}-order statistics are used, the joint probability matrix would have dimension $2(b+1)$. The individual entries would be denoted by

$$\mathrm{P}_{M,V}(m, v|\mathbf{m}_b, \mathbf{v}_b), \tag{6}$$

which is the joint probability of movement m and velocity v at time iT, given the past b observed movements and velocities.

Notice that the size of the probability matrix in the JMPVRW model grows twice as fast as the MPVRW model does for increasing b. Therefore, if the statistics of realistic movement and velocity are not strongly correlated, the MPVRW model may be used, since its complexity is less than that of the JMPVRW model, for a given b.

C. Comparing Mobility Models

The MPVRW and JMPVRW models are compared to other mobility models to determine whether the new models can capture more realistic human mobility. Specifically, the Gauss-Markov and the PVRW models are used as comparison mobility models.

Simulations are done on select paths of interest. The first path of interest results from the 2^{nd} 5 minutes of data collected of a non-disabled person moving about the experiment space at the Madonna Rehabilitation Center, which will be referred to as Path 1. The second path of interest was generated artificially in MATLAB, and will be referred to as Path 2. It is a simple path that is meant to mimic a model train moving on an oval track. This path is of interest since it has been used to measure the performance of smart space tracking algorithms in other work (e.g., [**?**]). The path's time duration is approximately 1.6 minutes. The third path results from the 5 minutes of data collected from a person using an electric wheelchair, and will be referred to as Path 3. Finally, the fourth path is the result of 5 minutes of data collected from a person using a cane. This path will be referred to as Path 4.

The first set of experiments investigates the statistical distributions of relative movements and quantized velocities for various human paths. For each path, the 1^{st}-order relative movement and quantized velocity statistics are gathered. These statistics represent the distributions of movement and velocity, given the previous movement and velocity. The purpose of this experiment is to determine the validity of the Gauss-Markov simulation model. Recall that in the Gauss-Markov model, 1^{st}-order statistics have a Gaussian distribution. Therefore, this experiment investigates how closely 1^{st}-order statistics gathered from the paths can be described by Gaussian distributions. For this experiment, let the prior relative movement index be denoted by $\mathrm{M}_{\text{prior}}$, and let the prior quantized velocity index be denoted by $\mathrm{V}_{\text{prior}}$.

The statistics were gathered for various paths and $F_s = \frac{1}{T}$, with the results plotted using MATLAB. The PMF of the relative movement requires some explanation, which is best done through example. In

the 9-state MPVRW case, relative movement 1 (forward) is mapped to the zero point on the horizontal axis. Relative movements 2, 3, 4, and 5 are mapped to 1, 2, 3, and 4 on the horizontal axis, and relative movements 6, 7, and 8 are mapped to -1, -2, and -3 on the horizontal axis. Relative movement 9 (no movement) is not plotted; in fact, the 'no movement' case is not counted in these statistics. Therefore these PMFs show the distribution of the relative movements when there *is* movement. The effect of this mapping, with respect to the Gauss-Markov comparison, is to ease visual analysis.

The statistics explored initially are derived from Path 1 with $F_s = 4$ Hz. Relative movement results can be seen in Figure 3 for the 33-state MPVRW. In addition to the experimental PMFs, a Gaussian PMF

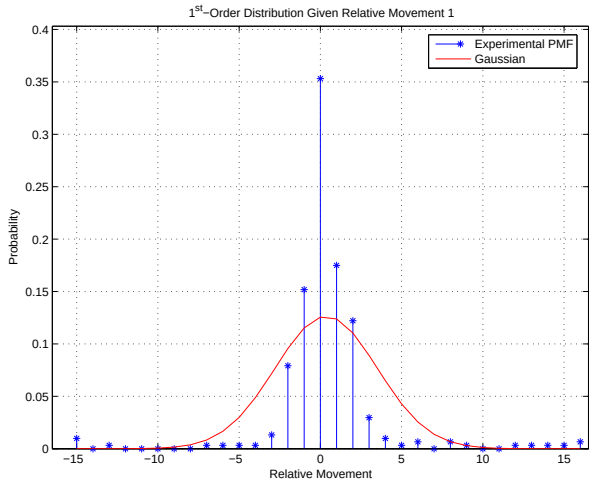

Fig. 3. 1^{st}-order Relative Movement Statistics for Path 1 with $F_s = 4$ Hz, $\mathrm{M}_{\text{prior}} = 1$.

is also plotted, with mean and variance equal to the experimental mean and variance. Although it is a PMF, it is plotted with a continuous line to ease visual analysis. Quantized velocity results can be seen in Figure 4. Normality plots are shown in Figures 5 and 6 for the movement and velocity statistics. Note

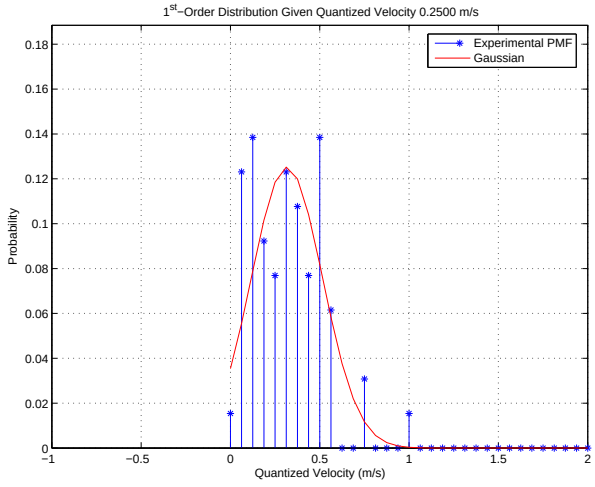

Fig. 4. 1^{st}-order Quantized Velocity Statistics for Path 1 with $F_s = 4$ Hz, $\mathrm{V}_{\text{prior}} = 5$.

that if the data is normally (Gaussian) distributed, the data points will plot closely to the linear line in a normality plot.

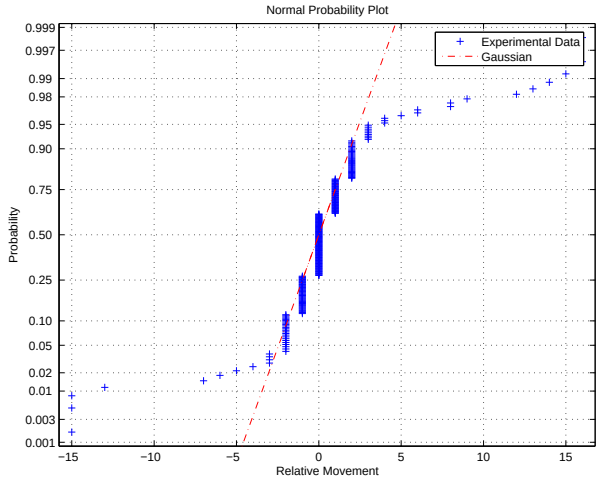

Fig. 5. Normality Plot for Path 1 with $F_s = 4$ Hz, $\mathrm{M}_{\mathrm{prior}} = 1$.

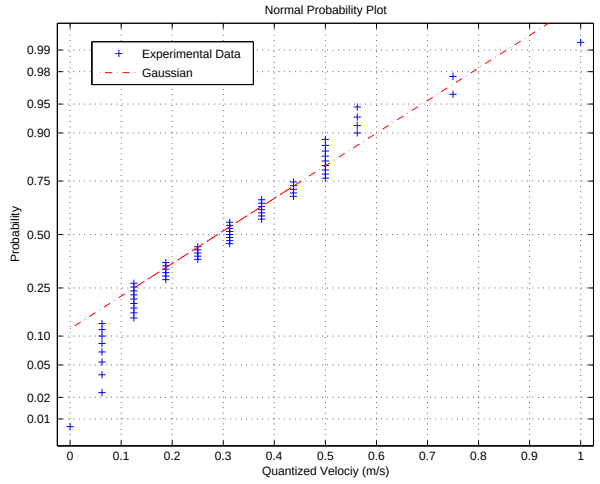

Fig. 6. Normality Plot for Path 1 with $F_s = 4$ Hz, $\mathrm{V}_{\mathrm{prior}} = 5$.

The statistics explored second are derived from Path 2 with $F_s = 4$ Hz. The purpose of showing Path 2's statistics is to present how much they differ from statistics collected from actual human mobility. Results can be seen in Figures 7 and 8 for the 33-state MPVRW.

It was found experimentally that three parameters affect the distributions: previous state, mobility type, and sampling frequency.

The 1^{st}-order distribution of relative movements depends upon the previous relative movement. As the previous movement gets farther away from the forward direction, the distribution appears to become more uniform. Also, when the previous movement is the 'no movement' case, the distribution is very different from the other distributions.

When the previous movement is forward, the distribution is seen to be highly centralized about the forward movement, as seen in Figure 3. This distribution is non-Gaussian.

Recall that in the Gauss-Markov model, conditional distributions are identical for all conditions, only with a shift in the mean. Thus, the Gauss-Markov model is an inaccurate mobility model for movement directions. Not only do these experiments show that the conditional distributions are dependent upon the previous movement, but they also show that the distributions are non-Gaussian.

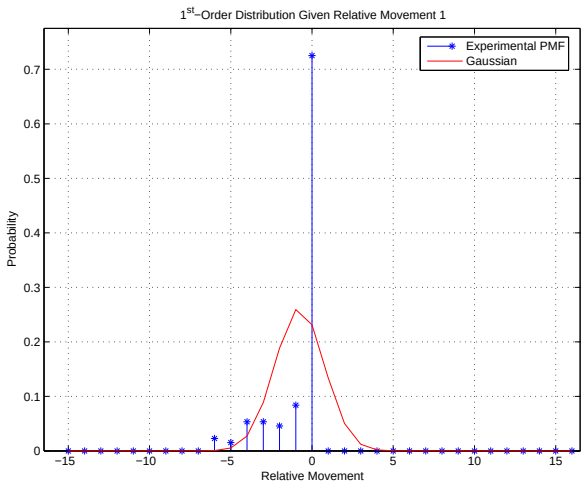

Fig. 7. 1^{st}-order Relative Movement Statistics for Path 2 with $F_s = 4$ Hz, $\mathrm{M}_{\text{prior}} = 1$.

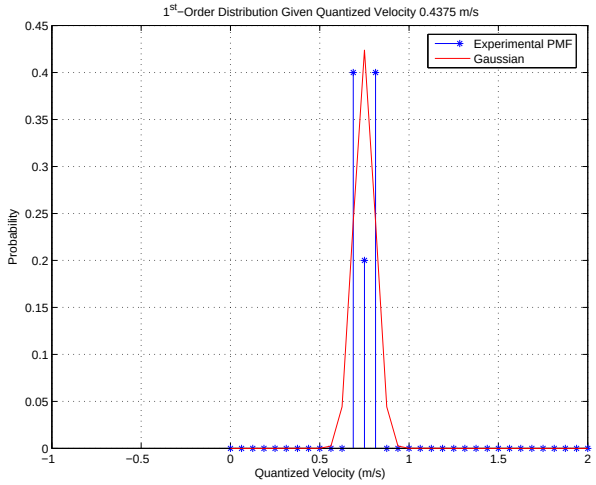

Fig. 8. 1^{st}-order Quantized Velocity Statistics for Path 2 with $F_s = 4$ Hz, $\mathrm{V}_{\text{prior}} = 1$.

Experiments also show that the conditional distribution of quantized velocities depends upon the previous velocity. In addition, it can be seen that when the previous velocity is close to zero, as it is in Figure 4, the distribution cannot be truly Gaussian, as the velocity is not allowed to be less than zero. In these cases, simulations show that the distribution is closer to a truncated Gaussian, similar that that seen in Figure 4. However, it was found experimentally that as the previous velocity continues to increase beyond zero, the distribution can be approximated by a Gaussian.

Although the Gaussian model may describe the conditional distribution of the quantized velocities in some cases, it is not able to describe it in all cases. Therefore, the Gauss-Markov model is also an inaccurate mobility model for velocities.

The 1^{st}-order distributions obtained from Path 2 can be seen in Figure 7. These distributions show the difference between real human mobility and train mobility. The simulated train movements and velocities have less variety than those from the human paths. Additionally, the simulated train distributions have very different forms than those found in human paths. The significance of this lies in predicting the performance of tracking algorithms. In this application, performance is often determined for simple train-like paths,

and the results are used to predict tracking performance of real people. However, as these experiments show, human mobility is very different from train-like mobility. Thus, tracking performance of train-like paths may not be a good indicator of tracking performance of human paths.

Although not shown here, the effects of sampling frequency on the relative movement and quantized velocity distributions were found to be significant for all of the paths. Experiments show that the resulting distributions at $F_s = 1$ Hz are generally less centralized than those found at $F_s = 4$ Hz. In other words, the distributions become more 'random'. This trend continues as sampling frequency gets even lower.

Thus, this shows that sampling frequency has a strong effect on the conditional distributions. Therefore, in the context of evaluating mobility models, sampling frequency must be considered when determining the accuracy of mobility models. For example, the Gauss-Markov model is shown to be somewhat accurate in describing the conditional distribution of velocity. However, experiments show that decreasing the sampling frequency causes the Gauss-Markov model to be less accurate in describing the conditional distribution of velocity.

Next, simulations are performed to investigate the amount of memory that the statistics have for the various paths. This is done by investigating the predictive effectiveness of different order statistics. The 17-state static predictive MPVRW model is used to predict paths by making use of those paths' statistics (e.g., Path 1 is predicted using Path 1's statistics) as explained in [**?**]. For these simulations, the predictor is allowed perfect knowledge of past movements and velocities before it makes each prediction.

The metric of interest for these simulations is Mean Square Error Ratio (MSER). Suppose the prediction of the mobile node's position at time iT is $(\hat{x}_i^-, \hat{y}_i^-)$, and the mobile node's true position is (x_i, y_i). For a path with L sample points and sampling frequency F_s, MSER is defined to be

$$\text{MSER} = \frac{1}{Ld_{\text{ave}}^2} \sum_{i=0}^{L-1} \left(\left(x_i - \hat{x}_i^- \right)^2 + \left(y_i - \hat{y}_i^- \right)^2 \right), \tag{7}$$

where d_{ave} is the average distance traveled by the mobile node from one sampling instant to the next. The normalization is done so that performance can be compared for different sampling frequencies.

In theory, a predictor with $(b+1)^{\text{th}}$-order statistics should not perform better than a predictor using b^{th}-order statistics, if the path only has memory b. That is, using more than b past movements and velocities should provide no more information about the next movement and velocity than using b past movements and velocities (i.e., the path is defined by a b^{th}-order Markov model). This is formally defined by:

$$\text{P}_M(m|\mathbf{m}_b) = \text{P}_M(m|\mathbf{m}_\infty) \tag{8}$$

$$\text{P}_V(v|\mathbf{v}_b) = \text{P}_V(v|\mathbf{v}_\infty), \tag{9}$$

where $\mathbf{m}_\infty$ is all past relative movements, and $\mathbf{v}_\infty$ is all past quantized velocities.

The MSER is found for various values of b and F_s for each path, and results are plotted using MATLAB. The first path investigated is Path 1; results are shown in Figure 9 for $F_s = 1$ Hz and $F_s = 4$ Hz.

The second path investigated is Path 2. Results for $F_s = 1$ Hz and $F_s = 4$ Hz are shown in Figure 10.

Path 1 seems to have memory up to at least order 5, as seen in Figure 9. Simulations show that as b increases from 0 to 5, MSER decreases. For $F_s = 4$ Hz, this decrease is sharp going from $b = 0$ to $b = 1$. However, as b increases beyond 1, the decrease in MSER is more gradual. When $F_s = 1$ Hz, the decrease in MSER with increasing b is fairly sharp going from $b = 0$ to $b = 4$, but is much more gradual going from $b = 4$ to $b = 5$. Similar results are found for Path 3 and Path 4. However, for Path 3 at $F_s = 4$ Hz, the decrease in MSER is even more gradual after $b = 1$ than for the other human paths.

Clearly, memory is more important at $F_s = 1$ Hz than at $F_s = 4$ Hz. At $F_s = 1$ Hz, using more memory provides a steady improvement in MSER, up to $b = 4$. However, at $F_s = 1$ Hz, using more memory provides only moderate improvement in MSER once b increases beyond 1.

Based on these results, the PVRW model may not be an accurate model for realistic human mobility. Recall that the PVRW model only has memory 1. When $F_s = 4$ Hz, this may not be a bad approximation to realistic human mobility. However, when $F_s = 1$ Hz, the approximation that human paths have only

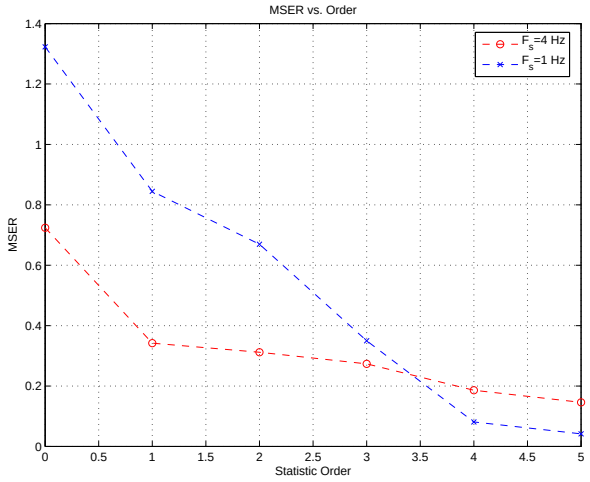

Fig. 9. Prediction MSER for Path 1.

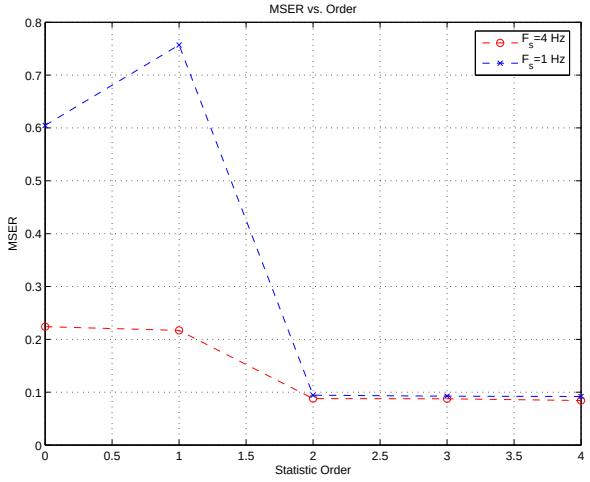

Fig. 10. Prediction MSER for Path 2.

memory 1 is not accurate. Therefore, sampling frequency has a role in determining the accuracy of a mobility model, and should be considered.

Figure 10 shows that Path 2 seems to have less memory than Path 1. This is seen in the leveling off of MSER as b increases beyond 2. Therefore it seems that Path 2 has memory 2, since using higher-order statistics does not noticeably improve MSER. This is true for both $F_s = 4$ Hz and $F_s = 1$ Hz. This low memory should be expected from inspection of Path 2. This path is not very complex, as it repeats itself over and over. The effect of low complexity is to allow lower-order statistics and higher-order statistics to be able to describe the path equally well. This result can be used as a guide for determining what order statistics are needed to accurately model a given mobility type. Based on these results, if a mobility type is suspected to have low complexity, then higher-order statistics may not be needed to achieve a desired accuracy. Conversely, if a mobility type is suspected to be complex, then higher-order statistics may be needed.

Experiments are performed to investigate the dependence of relative movements and quantized velocities. For each path, the 9-state JMPVRW's 0^{th}-order joint statistics are gathered. These are used to calculate the correlation coefficient, $\rho_{M,V}$. Note that correlation is calculated for the non-zero velocities and the

all relative movements except the 'no movement' case. The zero velocity and 'no movement' states are excluded since they always occur simultaneously (since they are simply two different ways of stating the same movement), and so would cause the magnitude of $\rho_{M,V}$ to be larger than desired, thus implying more dependence between relative movement and quantized velocity than actually exists. This is done for several input paths with $F_s = \frac{1}{2}$ Hz and $F_s = 4$ Hz. Dependence is shown by demonstrating that the independence of movements and velocities assumption is false. In terms of the correlation coefficient, independence implies $\rho_{M,V} = 0$. Note that $|\rho_{M,V}| \leq 1$.

For Path 1, the correlation coefficient is found to be -0.1966 for $F_s = \frac{1}{2}$ Hz, and -0.3261 for $F_s = 4$ Hz. Similar results are found for Path 4. However, Path 3 has a much smaller correlation for $F_s = 4$ Hz, i.e., $\rho_{M,V} = -0.08$. It seems that regardless of sampling frequency, human mobility has a dependence between relative movements and quantized velocities.

In comparing the results of $F_s = \frac{1}{2}$ Hz and $F_s = 4$ Hz, it appears that there is more dependence between relative movement and quantized velocity for $F_s = 4$ Hz. This agrees with the discussion of sampling frequency effects on conditional distributions. In that discussion, it was shown that the independent distributions become more random as sampling frequency decreases. A similar effect appears in the dependent distributions. As sampling frequency decreases, relative movements and quantized velocities are less dependent upon each other, (i.e., they are more 'random' with respect to each other). This observation is confirmed in the correlation coefficients, where a lower sampling frequency results in a smaller absolute value of $\rho_{M,V}$. The exception is electric wheelchair mobility. For higher sampling frequency, the relative movements are almost entirely the forward case, while the velocities still have a distribution. This explains the lack of a large correlation between movement and velocity for the wheelchair mobility at higher sampling frequencies.

Based on these results, it may not be accurate for models to treat movement direction and velocity independently, as the PVRW and MPVRW models do. If this is the case, then a model such as the JMPVRW may be used to generate human mobility with the desired realism.

REFERENCES

[1] F. Jiang, E. Psota, and L. Perez, "Decoding turbo codes based on their parity-check matrices," pp. 221 –224, March 2007.

[2] N. Axvig, E. Price, E. Psota, D. Turk, L. Pérez, and J. Walker, "A universal theory of pseudocodewords," in *Proceedings of the 45th Annual Allerton Conference on Communication, Control, and Computing*, September 2007.

[3] N. Axvig, K. Morrison, E. Psota, D. Turk, L. C. Pérez, and J. L. Walker, "Average min-sum decoding of LDPC codes," in *2008 International Symposium on Turbo Codes and Related Topics*, September 2008.

[4] N. Axvig, D. Dreher, K. Morrison, E. Psota, L. Perez, and J. Walker, "Towards universal cover decoding," pp. 1 –6, December 2008.

[5] E. Psota and L. C. Pérez, "LDPC decoding and code design on extrinsic trees," in *Proceedings of the 2009 International Symposium on Information Theory*, June and July 2009.

[6] E. Psota and L. Perez, "Extrinsic tree decoding," in *Information Sciences and Systems, 2009. CISS 2009. 43rd Annual Conference on*, pp. 406 –410, March 2009.

[7] E. Psota and L. Perez, "Connections between problematic trapping sets and deviations on the computation trees of LDPC codes," in *Turbo Codes and Iterative Information Processing (ISTC), 2010 6th International Symposium on*, pp. 472 –476, September 2010.

[8] E. Psota, *Finite Tree-Based Decoding of Low-Density Parity-Check Codes*. PhD thesis, University of Nebraska-Lincoln, January 2010.

[9] A. Guha, E. Psota, and L. C. Pérez, "Non-binary joint network-channel decoding of correlated sensor data in wireless sensor networks," in *IEEE Wireless Communications and Networking Conference*, March 2011.

[10] N. Axvig, K. Morrison, E. Psota, D. Dreher, L. Pérez, and J. L. Walker, "Analysis of connections between pseudocodewords," *IEEE Transactions on Information Theory*, vol. 55, pp. 4099–4107, September 2009.

[11] E. Psota and L. C. Pérez, "The manifestation of stopping sets and absorbing sets as deviations on the computation trees of LDPC codes," *Journal of Electrical and Computer Engineering*, vol. 2010, no. Article ID 432495, p. 17, 2010.

[12] E. Psota and L. C. Pérez, "Iterative construction of regular LDPC codes from independent tree-based minimum distance bounds." To appear in *IEEE Communications Letters*, 2011.

[13] E. Psota and L. C. Pérez, "Finite tree-based decoding of low-density parity-check codes." To be submitted to *IEEE Transactions on Communications*, 2011.

[14] E. Psota and L. C. Pérez, "A deviation-based conditional upper bound on the error floor performance for min-sum decoding of LDPC codes." To be submitted to *IEEE Transactions on Information Theory*, 2011.

[15] Y. Tan, M. C. Vuran, and S. Goddard, "Event model for cyber-physical systems," in *Proceedings of the 29th IEEE International Conference on Distributed Computing Systems Workshops: The 2nd International Workshop on Cyber-Physical Systems (WCPS 2009)*, (Montreal, Canada), Jun 2009.

[16] Y. Tan, M. C. Vuran, S. Goddard, Y. Yu, M. Song, and S. Ren, "A concept lattice-based event model for cyber-physical systems," in *Proceedings of the ACM/IEEE First International Conference on Cyber-Physical Systems*, (Stockholm, Sweden), Apr 2010.

[17] Y. Wang, M. C. Vuran, and S. Goddard, "Cross-layer analysis of the end-to-end delay distribution in wireless sensor networks," in *Proc. IEEE RTSS '09*, (Washington, DC), Dec 2009.

[18] Y. Wang, M. C. Vuran, and S. Goddard, "Stochastic analysis of energy consumption in wireless sensor networks," in *Proc. SECON*, (Boston, MA), Jun 2010.

[19] Y. Wang, M. C. Vuran, and S. Goddard, "Analysis of event detection delay in wireless sensor networks," Tech. Rep. TR-UNL-CSE-2010-0007, Department of Computer Science and Engineering, University of Nebraska-Lincoln, 2010.